Nuclear Magnetic Resonance Spectra of TmVO$_4$ at Low Fields

D. Garcia

Physics Department, University of California, Davis

Low magnetic fields were utilized in collecting nuclear magnetic resonance (NMR) spectra of TmVO$_4$, in order to increase signal homogeneity. Having the proper conditions to create NMR signals with negligible or no line width will be necessary in future research involving the study of ferroquadrupolar ordering demonstrated by Tm. Spectra were collected at 2.14T and 1.43T. Cross-sectional and three-dimensional models of the demagnetization effects at both of these fields, shown as the internal magnetic field ($\vec{B}$) of the crystal at every point, were created in Mathematica. Histograms were made to identify the relationship between $\vec{B}$ field and the angle, and also the frequency and the angle. The experiment was able to successfully decrease the width in the NMR spectra lines by reducing $\vec{H}$. Following this experiment, an ellipsoid TmVO$_4$ crystal will be used in an attempt to further remove the effects of demagnetization.

I. INTRODUCTION

Thulium (Tm) is a rare earth metal, located in the f-block on periodic table. Rare earth metals are usually associated with their magnetic properties. However, Tm is unable to order magnetically and instead demonstrates electron orbital alignment. At higher temperatures, the available energy allows for changes in electronic energy levels, as well as different orientations of electronic spins directions. Once a low enough temperature is achieved, in order to minimize the energy, the electron orbitals all align in the same directions. This is called ferroquadrupolar ordering [6]. Under the proper conditions - below a temperature of 2.14 K and magnetic field of 0.8 T - Tm undergoes ferroquadrupolar ordering. This experi-
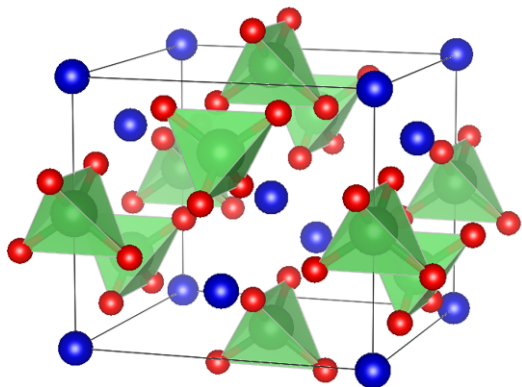

FIG. 2: The TmVO$_4$ crystal utilized, with dimensions in of 1mm $\times$ 1mm $\times$ 4mm.

FIG. 1: Unit cell of TmVO$_4$. The blue spheres represent the thulium molecules, the green tetragonal structures represent the vanadium bonded to the four oxygen molecules (the red spheres).

ment utilized a TmVO$_4$ crystal. Nuclear Magnetic Resonance (NMR) was used to study the properties of the crystal [1]. The large electron cloud of Tm made it difficult to obtain an NMR signal, seen in Figure 1 as the green pyramidal shape. instead, the signal from the Vanadium (V51) nuclei were measured. The nucleus of V51 is quadrupolar, with a spin of $\frac{7}{2}$. Due to quadrupolar and hyperfine interactions, the NMR signal produced by V51 is shifted and contains 7 peaks [2]. A
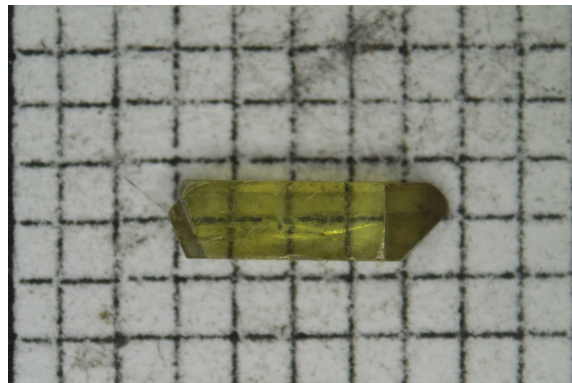
quadrupole is similar to a dipole, in which there is a positive and negative magnetic poles, but rather has four positive and four negative magnetic poles. The hyperfine interactions lies between the nucleus and the electron clouds, leading to small shifts in the energy levels. Demagnetization within the crystal produced a signal with peaks that were too broad, making it difficult to distinguish individual peaks. In order to minimize the line width, the crystal was rotated until it was aligned to exactly 90° from the applied external magnetic field. In conjunction with obtaining experimental data, the effects of demagnetization were also calculated, taking into account the material and exact dimensions of the crystal. The demagnetization effects were calculated at 2.14 T and 1.43 T.

Demagnetization of the magnetic field within the crystal causes the width in the NMR spectrum [3]. The width of the signal is determined at the half maximum of the center peak, also known as the full width half maximum (FWHM). A sphere or ellipsoid has a uniform internal field, thus producing lines with negligible or no width [7]. The field of a rectangular crystal, as seen in Figure 2, is nonuniform and bends at the edges. The level at which the field lines bend is dependent on the angle between the c-axis of the crystal and the external magnetic field. As a result, the nuclei at the edge of the crystal experience a different frequency from the nuclei in the center. The resonant frequencies of the nuclei result in the width of

the NMR lines. In order to achieve ferroquadrupolar ordering, the crystal needs to be perfectly aligned. Otherwise, the demagnetization would cause nuclei at the edges to become ordered and/or non-ordered before nuclei in the center.

II. EXPERIMENT

To conduct the experiment, a silver coil was made to fit the crystal. Silver was used to avoid any interference in the NMR signal. The coil was soldered onto a tank circuit, in place of the inductor seen in Figure 3. The circuit was at the end of a long probe, the opposite end containing two tuning rods, one for each capacitor. The probe was then placed into a
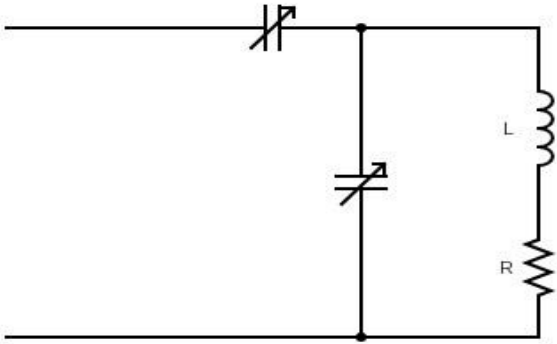

FIG. 3: Tank circuit consisting of two tuneable capacitors, a resistor (R) and an inductor (L).

PPMS magnet. The PPMS consisted of an adjustable magnet, encased in a layer of liquid helium, a vacuum layer, and a layer of liquid nitrogen. Any adjustments made to the field were followed by a frequency sweep. This involved taking multiple NMR signals to determine the frequency at which the strongest signal would be found. Then, a thorough, long-term NMR signal was collected. The relationship between the applied magnetic field and the frequency is:

$$f(x, y, z) = \gamma |\overrightarrow{B}(x, y, z)| \tag{1}$$

where f(x,y,z) is the frequency of the NMR signal in three-dimensions, gamma is the gyromagnetic constant, and $\overrightarrow{B}$(x,y,z) is the magnetic field vector [8]. The gyromagnetic constant is the ratio between a particle's magnetic moment and angular momentum. It is a value that is unique to each atomic species.

In conjunction with collecting experimental data the effects of demagnetization at every single point within the crystal were calculated using Mathematica, then used to create two dimensional cross-sections and three dimensional models [4] [5]. The exact dimensions of the crystal were measured and used in the calculations. Utilizing values for the applied magnetic field ($\overrightarrow{H}$), the magnetic moment ($\overrightarrow{M}$), and the susceptibility

(χ) of the crystal, the demagnetization tensor (D) was calculated:

$$\overrightarrow{M} = \chi \times \overrightarrow{H} \tag{2}$$

$$\overrightarrow{H} = D \times \overrightarrow{M} \tag{3}$$

Then the magnetic induction ($\overrightarrow{B}$) was calculated by substituting values into:

$$\overrightarrow{B} = \overrightarrow{H} + 4\pi\overrightarrow{M} = (\Gamma + 4\pi\chi\Gamma)\overrightarrow{H} \tag{4}$$

where

$$\Gamma = (1 - D\chi)^{-1} \tag{5}$$

Once the values for $\overrightarrow{B}$ were determined at every single point inside the crystal, they were used to construct cross-sections and 3-D models.

III. RESULTS

The first spectrum was taken at 2.14T. The peak signal was at approximately 24 MHz, as seen in Figure 4. The FWHM was calculated as about 0.05 MHz. The field was then brought down to 1.43T. The peak signal was at approximately 16 MHz, with the FWHM calculated to be about 0.025MHz, as seen in Figure 5. Decreasing the magnetic field by 0.71T resulted in a 0.025 MHz width reduction - nearly half of the original line width.
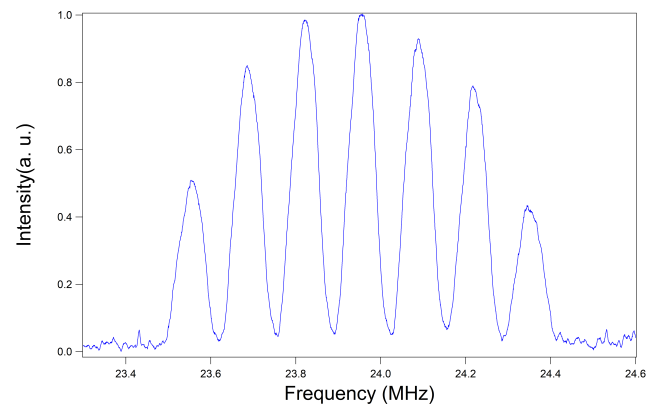

FIG. 4: NMR spectrum of TmVO$_4$ at a temperature of 100K and applied magnetic field of 2.14T. The FWHM was 0.048 MHz.

The cross-sections show the internal magnetic field ($\overrightarrow{B}$) of a single plane within the crystal at every single point, Figure 6. The bright yellow represents the areas of high fields, while the dark blue represent areas of low field. This demonstrates that the $\overrightarrow{B}$ is nonuniform through the crystal, an effect of demagnetization. When the c-axis of the crystal is perpendicular
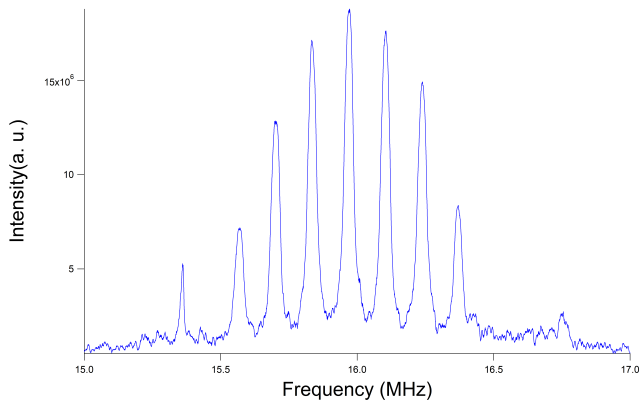
FIG. 5: NMR spectrum of TMVO$_4$ at a temperature of 210K and applied magnetic field of 1.43T. The FWHM was 0.025M MHz.

with the $\overrightarrow{H}$ field the largest fields are on the edges of the crystal and smallest in the center. The opposite is true for when the c-axis is parallel with the $\overrightarrow{H}$ field. It should be noted that while cross-sections were taken at 1.43T, the same effect is true at 2.14T.
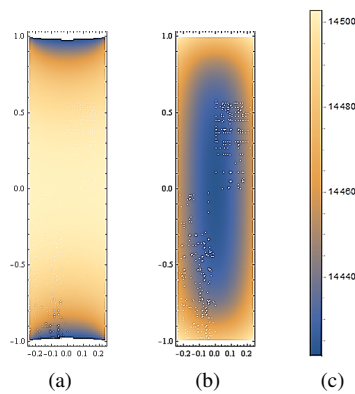

FIG. 6: Cross-sections of the internal magnetic field of the crystal in the c-plane at 14300 Gauss (1.43T). (a) c-plane 90° from the applied magnetic field, (b) c-plane 0° from applied magnetic field, (c) color scale of internal magnetic field ranging from 0-14500 Gauss. The units for the values on the axis for (a) and (b) are arbitrary. The values show that the center is at 0 and the edges extend evenly outward in every direction.

The models in three dimensions show the $\overrightarrow{B}$ field of multiple planes within the crystal, Figure 7. The color scheme is the same as the one for the cross-sections. The 3-D models are in agreement with the cross-sections, with the edges and the center containing different fields.

Once the values were collected, histograms were made showing the relationship between the ($\overrightarrow{B}$) field and the angle, seen in Figure 8. The histograms describe the number of spots in the sample with a given field magnitude. As the angle was increased, shifted from being parallel to perpendicular to the applied field, there was a decrease in the $\overrightarrow{B}$ field.
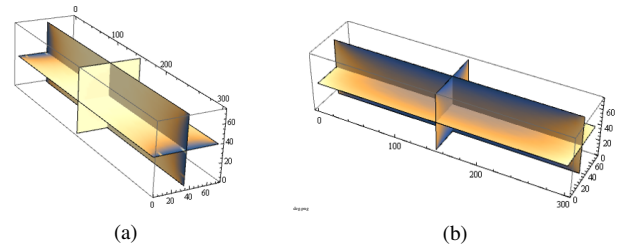

FIG. 7: Three-dimensional model of internal magnetic field of the crystal at 14300 Gauss (1.43T). (a) x-plane 0° from the applied magnetic field, (b) x-plane 90° from the applied magnetic field. The units for the values on the axis for (a) and (b) are arbitrary. The values show that the center is at 0 and the edges extend evenly outward in every direction.
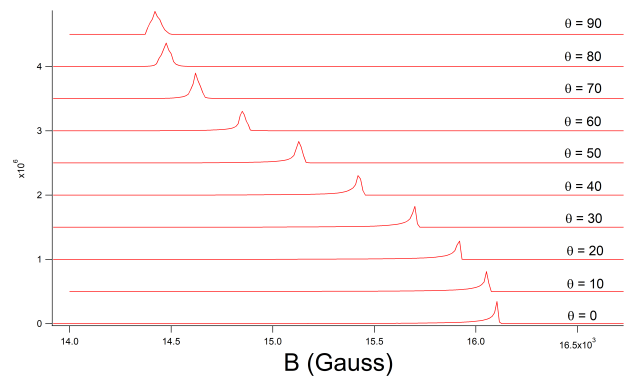

FIG. 8: Histograms of the angular dependence of the internal magnetic field (B), taken at 10° intervals.
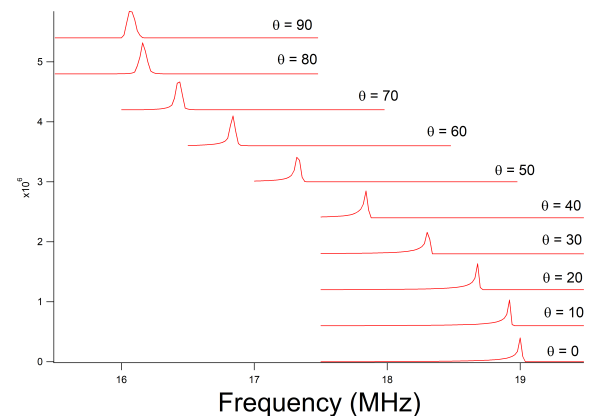

FIG. 9: Histograms of the angular dependence of the signal frequency (f), taken at 10° intervals.

Similarly, the relationship between the frequency (f) and angle is shown in Figure 9. The histograms show the number of spots in the sample with a given frequency. It can also be seen that f decreased as the angle changed from being parallel to perpendicular to the applied field. The lines in Figure 9 are incomplete as a result of a deliberate vertical offset.

IV. CONCLUSION

At 2.14T the FWHM was 0.048 MHz, and at 1.43T the FWHM was 0.025 MHz. In decreasing the $\vec{H}$ field by 0.7T, the FWHM was dropped to almost half of the initial width. However, the width of the signal was still significant. The models confirmed that the outer edges of the crystal experienced a $\vec{B}$ field different to that in the center, demonstrating the effects of demagnetization. These different internal fields lead to resonant frequencies and a broadened signal. The histograms showed that a perpendicular orientation of the crystal, Figures 6b and 7b, is more favorable. This produces the lowest $\vec{B}$ field and in order to achieve ferroquadrupolar ordering a low field is necessary. The next step involves utilizing an ellipsoid crystal. This should remove the effects of demagnetization, since spherical and ellipsoid objects don't experience the bending of the field lines seen at the edges of rectangular objects. If the crystal is oriented such that the c-axis is perpendicular to the $\vec{H}$, the ellipsoid should remove the high fields at the outer edges of the models and therefore the entire crystal would experience a uniform, low magnetic field.

[1] Curro, N. J., "Nuclear magnetic resonance as a probe of strongly correlated electron systems," *Strongly correlates systems: Experimental Techniques*, edited by A. Avella F. Mancini, New York, Springer, 1 (2015).

[2] Dioguardi, A., "NMR evidence for inhomogeneous nematic fluctuations in $BaFe_2(As_{1-x}P_x)_2$," *Phys. Rev. Lett.* **116**, 10 (2016).

[3] Dioguardi, A., "Nuclear magnetic resonance studies of the 122 iron-Based superconductors (Doctoral dissertation)," *University of California, Davis*, (2013).

[4] Griffiths, D. J., "Introduction to electrodynamics," *Pearson Education Inc.* **3rd ed.**, New York (1999).

[5] Jackson, J., "Classical electrodynamics," *Wiley* **3rd ed.**, New York (1999).

[6] Maharaj, A.V., "Transverse fields to tune an ising-nematic quantum critical transition," *PNAS* **114**, 51 (2017).

[7] Purcell, E. M. Morin, D. J., "Electricity and magnetism," *Cambridge University Press*, Cambridge (2013).

[8] Townsend, J., "A modern approach to quantum mechanics," *University Science Books*, Sausalito, Calif. (2000).